Journal of Clinical and Experimental Cardiology

Mori et al., J Clin Exp Cardiolog 2018, 9:7
DOI: 10.4172/2155-9880.1000594

Research Article Open Access

Acute Thrombogenicity and Vascular Response after Bioresorbable Vascular Scaffold Implantation: Evidenced from Porcine Coronary Model

Masayuki Mori, Kenji Sakata, Chiaki Nakanishi, Junichiro Yokawa, Hirofumi Okada, Masaya Shimojima, Shohei Yoshida, Tadatsugu Gamou, Kenshi Hayashi, Masakazu Yamagishi* and Masa-aki Kawashiri

Department of Cardiovascular and Internal Medicine, Kanazawa University Graduate School of Medicine, Japan

***Corresponding author:** Masakazu Yamagishi, Department of Cardiovascular and Internal Medicine, Kanazawa University Graduate school of Medicine, 13-1 Takara-machi, Kanazawa Ishikawa, 920-8641, Japan, Tel: 81-76-265-2259; Fax: 81-76-234-4210; E-mail: myamagi@med.kanazawa-u.ac.jp

Received date: July 11, 2018; **Accepted date:** July 16, 2018; **Published date:** July 20, 2018

Abstract

Background: Recent clinical data of bioresorbable vascular scaffolds (BVS) have generated concerns about scaffold thrombosis in acute phase. However, few data exist regarding the mechanism of scaffold thrombosis especially in acute phase.

Methods: Ten BVS were implanted in non-injured coronary arteries of 4 swine that were followed for either 2nd or 14th day. The BVS were implanted according to 3 different pressures (nominal, low, and high pressure). The optical frequency domain imaging (OFDI) examinations were performed just after deployment and before euthanasia. Histological evaluation of stented segments was also performed. In addition, morphometric analysis of the inflammation (graded as inflammation score 0 to 3) and the intimal fibrin content (graded as fibrin score 1 to 3) was assessed.

Results: OFDI images showed that BVS were covered with tissue like neointima which was containing heavy fibrin in HE images among 3 groups in both 2nd and 14th day models. The scanning electron microscope images showed that BVS were covered with very rough tissue associated with thrombus. The percentage of thrombus area was higher in low pressure model than those in others, although other parameters were not different among 3 groups on the 2nd and 14th day.

Conclusion: These results demonstrate that delayed response to appear the neointima in the presence of thrombus, fibrin and inflammatory cells can contribute to the occurrence of stent thrombosis in BVS. We suggest that importance of optimal deployment techniques for BVS.

Keywords: Bioresorbable vascular scaffold; Stent thrombosis; Optical frequency domain imaging; Inflammatory response

Introduction

Metallic drug-eluting stents (DES) are the current standard for coronary intervention of coronary artery disease even for large size coronary artery [1]. However, metallic DES has been associated with delayed vascular healing that can lead to late complications even at long-term follow up [2-4]. Bioresorbable vascular scaffolds (BVS; Abbot Vascular, Santa Clara, CA) has been expected as new treatment for coronary artery disease that could potentially alleviate such problems [5,6]. However, some concerns about an increased rate of scaffold thrombosis (ScT), although the randomized Absorb II and EverBio-2 trials suggest similar efficacy compared with DES [6,7].

Several reports have identified under sizing as a key factor for stent thrombosis in both bare-metal stents and DES [8,9]. Actually, optical coherence tomography revealed that ScT was caused by under-expansion of BVS [10]. Under these conditions, histopathology analysis of the thrombi showed fragments of fibrin and platelet-rich thrombus with variable number of trapped red blood cells. On the other hand, sub-acute thrombosis occurred despite good expansion and apposition of BVS in the presence of long strut overlap. The high strut thickness of BVS and bench observations increased thrombogenicity of thick-strut stents which are more pronounced at overlap site [11].

There are several reports that procedure related underexpansion, malapposition, exaggerated thrombogenicity and inflammation were considered as main mechanism of ScT [12]. However, few data exist regarding the mechanism of ScT and the cause of ScT in acute phase. Therefore, the aim of this study was to clarify the impact of procedure related mechanical factors and or biological factors on ScT in acute phase.

Methods

Animal study protocol

The animal study was approved by the Animal Care and Use Committee of Kanazawa University, and the experiments were conducted according to the "Basic Guidelines for Conduct of Animal Experiments" published by the Ministry of Health, Labor and Welfare, Japan.

BVS (n=10, length 23 mm and diameter 3.0 mm) consisted of an absorbable polymer being coated with absorbable polymer poly (d, L-lactide) containing everolimus, were implanted in non-injured coronary arteries of 4 swine that were followed until the 2nd or 14th day

(n=2, each time point) after implantation. The delivery system is comparable to the one used in XIENCE Alpine coronary stent system.

All swine were treated with aspirin (200 mg, Bayer, Land Nordrheine-Westfalen, Germany) and clopidogrel (300 mg, Sanofi Aventis, Gouda, The Netherlands) for pre-procedure. Aspirin (200 mg) and clopidogrel (75 mg) were administered daily until the end of the study. After being anaesthetized with ketamine (20 mg/kg intramuscularly), swine were maintained on general anesthesia with 2% halothane and oxygen. During experimental procedure, we carefully observed anesthesia situation to maintain appropriate sedation. Electrocardiogram and heart rate were continuously monitored by a polygraph recording system (OptiPlex755, Nihon-Kohden, Tokyo, Japan) throughout the entire procedure. Heparin (5000 IU) was administered *via* the left carotid artery through 7 Fr sheath, and 2000 IU were injected every hour.

BVS deployment was performed by the method previously described previous report [13]. Briefly, stent delivery catheters (6 Fr Heartrail II, AL-0.75, TERUMO, Tokyo, Japan) were inserted through the sheath and were advanced over the 0.035 guidewire to the left and right coronary artery orifice. After coronary angiography, a 0.014-inch guidewire was inserted into the coronary arteries and optical frequency-domain imaging (OFDI; LUNAWAVE, TERUMO) was performed to measure lumen diameter.

BVS were implanted according to 3 different pressure such as low (5 to 6 atm), nominal (7 to 8 atm) and high (12 to 15 atm) for 3 times to create different results in terms of stent areas. After BVS implantation, we also performed OFDI to evaluate injury of the artery. Each animal received 2 or 3 BVS in the coronary artery and each coronary artery was implanted with a single BVS. At the end of the study, OFDI was again performed to evaluate vascular response. Then, the hearts were harvested and processed for SEM and histological analysis. Under these conditions, we controlled anesthesia not to response animal pain.

Tissue preparation

The stented vessels and normal coronary artery were perfused with saline and perfusion-fixed with 4% formaldehyde. The stented vessels were embedded in GMA resin and N, N-dimethyl aniline. Sections (5-6 μm thick, for a total of 5 sections) were cut using a cemented tungsten carbide knife (RM2245, Leica, Germany), and stained with hematoxylin and eosin (New Histology Science Laboratory Corporation, Tokyo, Japan). The sections were evaluated with an optical microscope (BZ-9000, KEYENCE, Osaka, Japan).

The stented vessels for SEM were fixed with 2.5% glutaraldehyde containing PBS for 2 h and subsequently treated with a series of dehydration steps using graded ethanolic aqueous solutions (50%, 70%, 90%, 99%, 99%, 99% ethanol, 10 min each step), freeze-dried in t-butyl alcohol, then sputter-coated with platinum. SEM images were observed using JSM-5400 (JEOL, Nagoya, Japan) at an acceleration voltage of 10 kV.

OFDI analysis

The OFDI catheter was pulled buck at a speed of 40 mm/sec [14]. The imaging data saved in the console were converted into AVI files and then transferred for offline quantitative analysis. Quantitative software (LUNAWAVE Offline Viewer, TERUMO) was used for off-line OFDI analysis. The OFDI images were manually measured at every 1 mm length of the cross-sectional from distal. BVS/artery ratio was defined as long diameter BVS/long diameter of artery (average of distal and proximal). In the stent site, the thrombus area was defined as stent area-lumen area [14]. The percentage of thrombus area was defined as 100 × thrombus area/stent area [15].

Histological analysis

Histological evaluation included the measurement of thrombus area, the percentage of thrombus area. Thrombus areas were measured around the stent and above the inner membrane. The percentage of thrombus area was defined as 100 × thrombus area/stent area [15]. We also performed morphometric analysis of the inflammation, injury (graded as score 0 to 3), and intimal fibrin content scores (graded as score 1 to 3) were also assessed. These parameters were calculated according to the previous reports method [16,17]. The sum of these scores for each segment was divided by the total number of struts in the examined section. The histological parameters were measured with digital morphometry.

Results

BVS were successfully implanted in the coronary arteries of 4 swine. All animals survived after the procedure and remained healthy until the end of the study.

OFDI and histological images

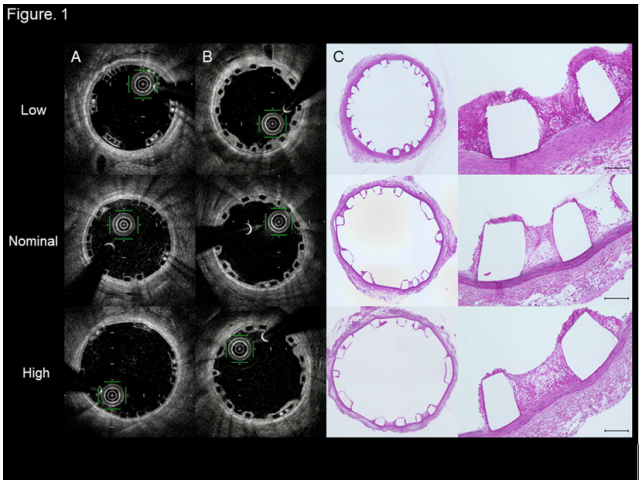

Figure 1: Representative OFDI and histological images on the 2nd day. Upper: Low pressure, Middle: Nominal pressure, Lower: High pressure, A: OFDI images just after deployment, B: OFDI images on the 2nd day, C: histological images (scale bar is 100 μm). OFDI images showed that some malappositioned struts were observed in low pressure Model, although almost struts were attached in nominal and high pressure model just after BVS deployment. BVS were covered with neointima in OFDI images, where a high intensity of BVS struts coverage. However, histological images revealed that BVS struts were surrounded with heavy fibrin deposition.

Just after BVS implantation, OFDI images showed that some malappositioned struts were observed in low pressure model, although almost struts were attached in nominal and high pressure models

(Figure 1A: upper, middle and bottom). On the 2nd day, the cross-sectional OFDI images demonstrated that all BVS were covered with neointima, where a high intensity of stent struts coverage was observed (Figure 1B: upper, middle and bottom). However, histological images revealed that stent struts were actually surrounded with heavy fibrin deposition and inflammatory cells (Figure 1C: upper, middle and bottom).

As for the 14th day model, there existed some malappositioned struts were observed in low pressure model, although almost struts were attached in nominal and high pressure models just after BVS implantation (Figure 2A: upper, middle and bottom). The cross-sectional OFDI images showed that all BVS were completely covered with tissue like neointima in 3 groups (Figure 2B: upper, middle and bottom). The histological images showed that the tissue was containing mainly fibrin deposition and inflammatory cells, suggesting presence of thrombus (Figure 2C: upper, middle and bottom).

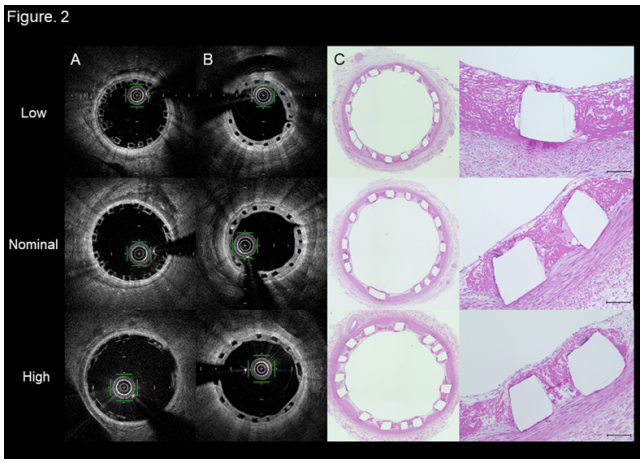

Figure 2: Representative OFDI and histological images on the 14th day. Upper: Low pressure, Middle: Nominal pressure, Lower: High pressure, A: OFDI images after deployment, B: OFDI images on the 2nd day, C: histological images (scale bar is 100 μm). OFDI images showed that some malappositioned struts were observed in low pressure model just after BVS deployment. BVS were completely covered with tissue like neointima in OFDI images which is containing fibrin and inflammatory cells in histological images.

SEM images showed that the BVS were partially covered with thrombus which was mainly observed around the BVS. Their surfaces seemed to be rough on the 2nd day (Figure 3A). On the 14th day, SEM images showed that BVS was mostly covered with thrombus whose surfaces were very rough. Under these conditions, blood cells and collagen tissue seem to be existed (Figure 3B).

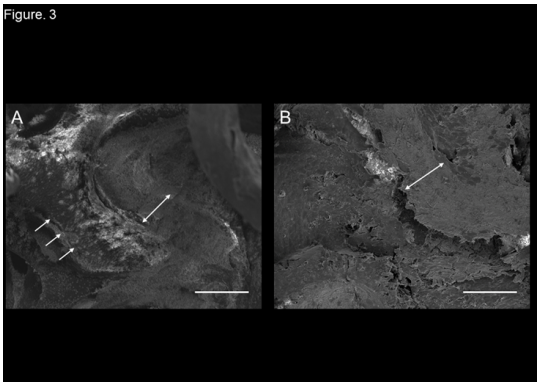

Figure 3: Representative scanning electron micrography images at low pressure model. On the 2nd day (A), the thrombus (unidirectional arrows) was mainly observed around BVS strut (bidirectional arrow). Their surfaces seemed to be rough. On the 14th day (B), all the BVS strut (directional arrow) and surrounding space were covered with asperous tissue where blood cells and collagen tissue seemed exist. Scale bar is 20 μm.

OFDI and histological analysis

Stent area and BVS/artery ratio were smaller in the low pressure group than in the high pressure group post procedure in both the 2nd and 14th day models (Table 1). Thrombus area assessed by both OFDI and histology did not differ among the 3 groups on the 2nd and 14th days (Table 1, 2). Thus, the percentage of thrombus area was higher in the low pressure model than that in the other groups, although other parameters did not differ among all models on the 2nd and 14th days. Furthermore, the fibrin content and inflammatory score did not differ among the 3 groups, either on the 2nd or 14th days (Table 2). Importantly, the injury score was negative in the 3 groups on the 2nd and 14th days, suggesting that the vessel injury was a consideration.

	After implantation		2nd day		
	Stent area (μm²)	BVS/artery ratio	Thrombus area (μm²)	Lumen area (μm²)	% Thrombus area (%)
Low	4	0.9	1	3.8	15.8
Nominal	5.2	1.1	0.9	4.8	14.5
High	5.8	1.5	1	5.1	14.6
	After implantation		14th day		
	Stent area (μm²)	BVS/artery ratio	Thrombus area (μm²)	Lumen area (μm²)	% Thrombus area (%)
Low	3.6	0.9	1.5	2.9	34
Nominal	4.8	1.2	1.6	3.8	27
High	5.1	1.4	1.7	4.5	25

Table 1: Result of OFDI analysis.

2nd day					
	Thrombus area (μm²)	**% Thrombus area (%)**	**Inflammatory score**	**Fibrin content score**	**Injury score**
Low	0.4	5.2	2.22	2.67	0
Nominal	0.4	4.3	2.18	2.61	0
High	0.3	4	2.1	2.6	0
14th day					
	Thrombus area (μm²)	**% Thrombus area (%)**	**Inflammatory score**	**Fibrin content score**	**Injury score**
Low	1.3	22	2.24	2.87	0
Nominal	1.1	17.5	2.21	2.79	0
High	0.9	15.6	2.05	2.73	0

Table 2: Result of histological analysis.

Discussion

The major findings of our study were as follows 1) the tissue like neointima which was observed by OFDI was thrombus containing fibrin; 2) thrombus area, fibrin content and inflammatory score were not different in spite of deployment techniques; 3) endothelialization could be impaired by heavy fibrin deposition and high inflammatory reaction. These data demonstrate that the presence of thrombus containing fibrin and associated deployed endothelialization can contribute to acute and sub-acute stent thrombosis in BVS.

OFDI is a highly promising tool for accurate evaluation of coronary stent strut coverage, as supported by a high agreement between OFDI and histological analysis. Therefore, OFDI analysis will provide important information on the biocompatibility of coronary stents [18]. In the present study, BVS seemed to be covered with neointima, where a high intensity of stent strut coverage. However, histological images revealed that there existed thrombus containing fibrin. Thus, there was a discrepancy in the results between OFDI and histological images. One of the explanations for this discrepancy was that the distinction of thrombus or neointimal coverage by OFDI might be difficult for property evaluation, although OFDI has a capacity to detect coronary stent struts coverage compared with IVUS analysis.

The procedure related underexpansion, malapposition and inflammation were considered as main mechanism of ScT by exaggerated thrombogenicity [12]. Early ScT were presumably because of procedural factors (underexpansion, undersizing, geographical miss). We implanted BVS according to 3 different pressures such as low, nominal and high ones to evaluate the procedure related mechanical factors and/or biological factors on ScT on acute phase. As a result, stent area and BVS/artery ratio were smaller in low pressure group than in high pressure group at post procedure, although the absolute thrombus area, fibrin content and inflammatory score were not different among 3 groups either 2nd or 14th day models. This suggests that BVS implantation in small lumen can be a high risk of ScT compared with large lumen.

We previously demonstrated that neointimal proliferation with endothelial cells starts 2 days after Biolimus A9 eluting stent implantation, and that stent struts were completely covered with neointima within 14 days in the same porcine coronary model [19]. The neointimal healing including inflammatory reaction with Biolimus A9 eluting stent was similar compared with bare-metal stent [19,20]. It is quite interesting that there were few thrombus, fibrin and inflammatory cells in comparison with those of BVS examined in the present study. The heavy fibrin deposition and adherence of inflammatory cells in acute phase frequently occur in BVS compared with second generation DES [21].

Actually, on the 2nd day, BVS were partially covered with thrombus which was containing heavy fibrin deposition and high inflammatory cells aggregation in histology. Importantly, the heavy fibrin deposition and high inflammatory cell aggregation continued on the 14th day. The neointimal healing process with BVS could be impaired by these heavy fibrin deposition and high inflammatory reaction. Clinically, the delayed stent healing with heavy fibrin deposition and fibrin coverage of stent struts has been observed with an increased risk of stent thrombosis [22,23]. In addition to the importance of obtained lumen area after BVS, our results demonstrate that clinical ScT in acute phase is associated with heavy fibrin deposition and high inflammatory reaction.

Limitation

There remain several limitations. First, we revealed vessel response to BVS in healthy conditions without atherosclerosis, because only healthy swine not suffering from arteriosclerosis were used for examination. Therefore, our findings have to be interpreted with caution when it comes to extrapolation to arteriosclerotic disease. Second, we did not perform statistical processing because the number of sample was very small. Further studies will necessary to confirm the present results.

Conclusions

In the present study, we demonstrated that delayed response to appear the neointima in the presence of thrombus, fibrin and inflammatory cells can contribute to the occurrence of stent thrombosis in BVS. We also demonstrate that expanded lumen size contributes to the percentage of thrombus area associated with stent thrombosis in BVS.

References

1. Yoshida T, Sakata K, Nitta Y, Taguchi T, Kaku B, et al. (2016) Short- and long-term benefits of drug-eluting stents compared to bare metal stents even in treatment for large coronary arteries. Heart Vessels 31: 635-642.
2. Guagliumi G, Sirbu V, Musumeci G, Gerber R, Biondi-Zoccai G, et al. (2012) Examination of the in vivo mechanisms of late drug-eluting stent thrombosis: findings from optical coherence tomography and intravascular ultrasound imaging. JACC Cardiovasc Interv 5: 12-20.
3. Amabile N, Souteyrand G, Ghostine S, Combaret N, Slama MS, et al. (2014) Very late stent thrombosis related to incomplete neointimal coverage or neoatherosclerotic plaque rupture identified by optical coherence tomography imaging. Eur Heart J Cardiovasc Imaging 15: 24-31.
4. Alfonso F, Dutary J, Paulo M, Gonzalo N, Pérez-Vizcayno MJ, et al. (2012) Combined use of optical coherence tomography and intravascular ultrasound imaging in patients undergoing coronary interventions for stent thrombosis. Heart 98: 1213-1220.

5. Karanasos A, Simsek C, Gnanadesigan M, van Ditzhuijzen NS, Freire R, et al. (2014) OCT assessment of the long-term vascular healing response 5 years after everolimus-eluting bioresorbable vascular scaffold. J Am Coll Cardiol 64: 2343-2356.
6. Serruys PW, Chevalier B, Dudek D, Cequier A, Carrié D, et al. (2015) A bioresorbable everolimus-eluting scaffold versus a metallic everolimus-eluting stent for ischaemic heart disease caused by de-novo native coronary artery lesions (ABSORB II): an interim 1-year analysis of clinical and procedural secondary outcomes from a randomised controlled trial. Lancet 385: 43-54.
7. Puricel S, Arroyo D, Corpataux N, Baeriswyl G, Lehmann S, et al. (2015) Comparison of everolimus- and biolimus-eluting coronary stents with everolimus-eluting bioresorbable vascular scaffolds. J Am Coll Cardiol 65: 791-801.
8. Fujii K, Carlier SG, Mintz GS, Yang YM, Moussa I, et al. (2005) Stent underexpansion and residual reference segment stenosis are related to stent thrombosis after sirolimus-eluting stent implantation: an intravascular ultrasound study. J Am Coll Cardiol 45: 995-998.
9. Okabe T, Mintz GS, Buch AN, Roy P, Hong YJ, et al. (2007) Intravascular ultrasound parameters associated with stent thrombosis after drug-eluting stent deployment. Am J Cardiol 100: 615-620.
10. Cuculi F, Puricel S, Jamshidi P, Valentin J, Kallinikou Z, et al. (2015) Optical Coherence Tomography Findings in Bioresorbable Vascular Scaffolds Thrombosis. Circ Cardiovasc Interv 8: e002518.
11. Karanasos A, van Mieghem N, van Ditzhuijzen N, Felix C, Daemen J, et al. (2015) Angiographic and optical coherence tomography insights into bioresorbable scaffold thrombosis: single-center experience. Circ Cardiovasc Interv 8: e002369.
12. Cuculi F, Puricel S, Jamshidi P, Valentin J, Kallinikou Z, et al. (2015) Optical Coherence Tomography Findings in Bioresorbable Vascular Scaffolds Thrombosis. Circ Cardiovasc Interv 8: e002518.
13. Takabatake S, Hayashi K, Nakanishi C, Hao H, Sakata K, et al. (2014) Vascular endothelial growth factor-bound stents: application of in situ capture technology of circulating endothelial progenitor cells in porcine coronary model. J Interven Cardiol 27: 63-72.
14. Nishimiya K, Matsumoto Y, Uzuka H, Oyama K, Tanaka A, et al. (2015) Accuracy of optical frequency domain imaging for evaluation of coronary adventitial vasa vasorum formation after stent implantation in pigs and humans - a validation study. Circ J 79: 1323-1331.
15. Sakata K, Waseda K, Kume T, Otake H, Nakatani D, et al. (2012) Impact of diabetes mellitus on vessel response in the drug-eluting stent era: pooled volumetric intravascular ultrasound analyses. Circ Cardiovasc Interv 5: 763-771.
16. Schwartz RS, Huber KC, Murphy JG, Edwards WD, Camrud AR, et al. (1992) Restenosis and the proportional neointimal response to coronary artery injury: results in a porcine model. J Am Coll Cardiol 19: 267-274.
17. Suzuki T, Kopia G, Hayashi S, Bailey LR, Llanos G, et al. (2001) Stent-based delivery of sirolimus reduces neointimal formation in a porcine coronary model. Circulation 104: 1188-1193.
18. Templin C, Meyer M, Müller MF, Djonov V, Hlushchuk R, et al. (2010) Coronary optical frequency domain imaging (OFDI) for in vivo evaluation of stent healing: comparison with light and electron microscopy. Eur Heart J 31: 1792-1801.
19. Mori M, Sakata K, Nakanishi C, Nakahashi T, Kawashiri MA, et al. (2017) Early endothelialization associated with a biolimus A9 bioresorbable polymer stent in a porcine coronary model. Heart vessels 32: 1244-1252.
20. Hagiwara H, Hiraishi Y, Terao H, Hirai T, Sakaoka A, et al. (2012) Vascular responses to a biodegradable polymer (polylactic acid) based biolimus A9-eluting stent in porcine models. EuroIntervention 8: 743-751.
21. Koppara T, Cheng Q, Yahagi K, Mori H, Sanchez OD, et al. (2015) Thrombogenicity and early vascular healing response in metallic biodegradable polymer-based and fully bioabsorbable drug-eluting stents. Circ Cardiovasc Interv 8: e002427.
22. Nakazawa G, Finn AV, Joner M, Ladich E, Kutys R, et al. (2008) Delayed arterial healing and increased late stent thrombosis at culprit sites after drug-eluting stent placement for acute myocardial infarction patients: an autopsy study. Circulation 118: 1138-1145.
23. Finn AV, Nakazawa G, Joner M, Kolodgie FD, Mont EK, et al. (2007) Vascular responses to drug eluting stents: importance of delayed healing. Arterioscler Thromb Vasc Biol 27: 1500-1510.